ASPEN

*Proc. of the 9th Intl. Conf. of Asian Society for Precision Engg. and Nanotechnology (ASPEN 2022)*
*15–18 November 2022, Singapore. Edited by* Nai Mui Ling Sharon and A. Senthil Kumar
doi://10.3850/978-981-18-6021-8_OR-11-0125

# Reduction of spherical aberration measurement error in high-numerical-aperture spherical test with synthetic-aperture Fizeau interferometry

**Toshiki Kumagai[1,2#], Keita Tomita[1], Kenichi Hibino[3] and Katsumi Wasaki[2]**

1 Olympus Corporation, Tatsuno, Kamiina-gun, Nagano 399-0495, Japan
2 Shinshu University, Wakasato, Nagano 380-8553, Japan
3 National Institute of Advanced Industrial Science and Technology, Tsukuba, Ibaraki 305-8567, Japan
# Corresponding Author / Email: toshiki.kumagai@olympus.com , TEL: +81-266-41-4219, FAX: +81-266-41-4245

KEYWORDS: Phase measurement; Phase-shift algorithm, Synthetic aperture, Fizeau interferometer.

*In spherical surface tests with conventional optical Fizeau interferometers, phase modulation within the observing aperture becomes spatially nonuniform due to geometrical effects. The phase increment decreases by -50% in the marginal regions when the numerical aperture of the test spherical surface reaches 0.86, which causes systematic errors in the measured surface profile. Even the recently developed error-compensating phase-shift algorithms suffer from induced spherical aberration with a magnitude of a few nanometers. We divided the aperture into several annular regions and applied different phase-shift analyses for different phase steps to each region. The new technique decreases the modulation nonuniformity from -50% to -8%. To prove the validity of the new method, the source wavelength was slightly shifted to change the initial phase of the object interference fringes. The induced spherical aberration errors were measured and compared for the conventional algorithm, the present synthetic method, and a wavelength tuning method.*

## 1. Introduction

Demand for high numerical-aperture (NA) spherical lenses is increasing for wide-angle or high-magnification optical products such as endoscopes, microscopes, and cameras. Measuring the surface shape of a spherical lens is performed using Fizeau interferometers, especially those with a mechanical phase shift.

The dominant error in these interferometers is ripple noise caused by an incremental error in the phase shift. This error has been reduced by several techniques, such as making the algorithm robust against phase-shift increments, calibrating the phase-shift increments, suppressing disturbance due to vibration and air turbulence, and measurement with null-fringe alignment.

The spatial nonuniformity of phase modulation is inherent in a monochromatic spherical interferometer. Figure 1 shows an optical setup for testing a spherical concave surface. The monochromatic beam from the source is collimated and illuminates the reference and test surfaces. The reference surface is translated along the optical axis by a piezo-electric transducer (PZT) to introduce phase modulation. However, because the oblique illuminating beams are not parallel to the translation direction, the phase modulation at each position of the aperture decreases by $\cos\theta$ where $\theta$ is the angle between the illuminating beam and the optical axis. The fringe modulation speed is therefore proportional to $\cos\theta$ and dependent on the position in the aperture. This modulation nonuniformity causes a significant phase measurement error in high-NA spherical testing [1]. The phase error exceeds a root-mean-square error of 1 nm for a NA ($\sin\theta$) of 0.7 and 4.5 nm for a NA of 0.86. In particular, the phase-shift nonuniformity becomes -50% for NA = 0.86, which overlaps the frequency of the 2nd harmonic interference signal with that of the fundamental signal.

We previously proposed a synthetic calculation [2] in which the observation aperture was divided into several annular regions, and the object phase in each region was calculated by an algorithm designed for the typical value of the phase modulation in each region. This technique decreased the maximum modulation nonuniformity from -50% to -8%. In this study, we quantitatively evaluated the aberration error in the spherical test and proved the validity of the synthetic approach.

Because the modulation nonuniformity is cylindrical around the optical axis, the resultant phase measurement error is also axially symmetric. A large part of the measurement error is reduced as a defocus component, which does not deform the object shape. However, some part of the error results in a spherical aberration that becomes a shape measurement error. The phase measurement error $\Delta\varphi$ is generally a periodic function of the object phase $\varphi$ and is denoted by

$$\Delta\varphi = J\varepsilon_1 \sin 2\varphi + K_0\varepsilon_2 + K_1\varepsilon_2 \cos 2\varphi$$
$$+ L_1 R\varepsilon_1 \sin\varphi + L_2 R\varepsilon_1 \sin 3\varphi \, , \#(1)$$

where $\varphi(x, y)$ is the measured object phase; $\varepsilon_1 = \cos\theta - 1$ is the phase modulation nonuniformity; $\varepsilon_2$ is the 2nd-order PZT extension nonlinearity; $R$ is the average reflection index for the surfaces; and $J$, $K_i$, and $L_i$ are the lowest-order error coefficients [3].

The magnitude of phase measurement error $\Delta\varphi$ can be estimated if we can uniformly change the initial value of the object phase $\varphi$. In a monochromatic interferometer, the initial phase variation can be introduced if we mechanically shift the initial position of the reference surface with the PZT. However, the translation also strays from the concentric positioning of null-fringe alignment, which can introduce additional aberration of the imaging optics into the measured object phase.

In this study, we used a tunable diode laser source and slightly changed the source wavelength (632.82–632.83 nm) to introduce a spatially uniform bias into the object phase. We measured the phase error $\Delta\varphi$ and calculated the resultant spherical aberration error in the object profile. We compared the results measured by three different methods using a conventional algorithm, the synthetic aperture method, and a wavelength tuning measurement.

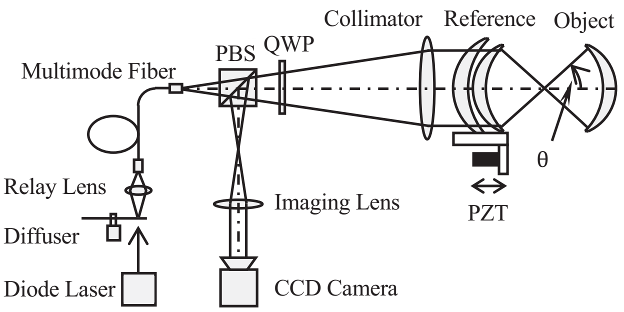


Fig. 1. Optical setup for spherical phase-shift Fizeau interferometer (PBS: polarization beam splitter, QWP: quarter-wave plate, PZT: piezoelectric transducer).

## 2. Experiments

A glass spherical concave surface with a diameter of 17 mm and NA = 0.86 was compared to a reference transmission concave surface with a diameter of 38 mm and the same NA. The optical setup of the measurement is shown in Fig. 1. The source was an external cavity diode laser with a wavelength $\lambda$ = 633 nm (Newport TLB-6804). The output beam from the laser was transmitted through a rotating ground glass diffuser and a multi-mode fiber to reduce the lateral coherence. The beam was then transmitted through a polarization beam splitter and a quarter-wave plate and collimated to illuminate the reference and test surfaces. The reflections from both surfaces retraced the same path and were reflected by the polarization beam splitter to generate interference fringes on a CCD detector (IMPERX, GEV-B1621W-TC0 1632×1232 pixels).

The reference surface was translated toward the object surface by a distance $\lambda$ and 13 interference images were recorded at equal phase-shift intervals of $\pi/3$. The object phase distribution $\varphi(x, y)$ was calculated by a single 13-frame error-compensating algorithm [3] over the whole aperture (hereafter, the conventional method). Second, the object phase was also calculated using the same interference images region by region using seven algorithms that were designed with phase steps of $2\pi/6$, $2\pi/7$, $2\pi/8$, $2\pi/9$, $2\pi/10$, $2\pi/11$, and $2\pi/12$ rad (hereafter, the synthetic aperture method). After calculating the object phase by the conventional method and synthetic aperture method, the source wavelength was slightly changed so that the object phase was shifted by $2\pi/40$ rad, and the same image recording and phase calculation were repeated. The initial phase variations were repeated 40 times over $2\pi$ rad. Figure 2 shows some of the 7th interference images in each measurement and the corresponding calculated object phase.

As another comparison, the source wavelength was tuned to modulate the interference fringes by 2 periods (632.82–632.83 nm), not translating the reference surface mechanically, and recording 13 interference images with an equal phase shift interval. The object phase was then calculated by the same 13-frame algorithm as used in the conventional method. The initial phase was shifted similarly step by step over $2\pi$ rad, and the measurement was repeated 40 times. Figure 2 shows some of the object phases calculated by the wavelength tuning method.

The object phase distributions obtained by the PZT mechanical modulation shown in Fig. 2 can involve systematic errors caused by the spatial nonuniformity of modulation. The phases were expanded into 36 Zernike polynomial components.

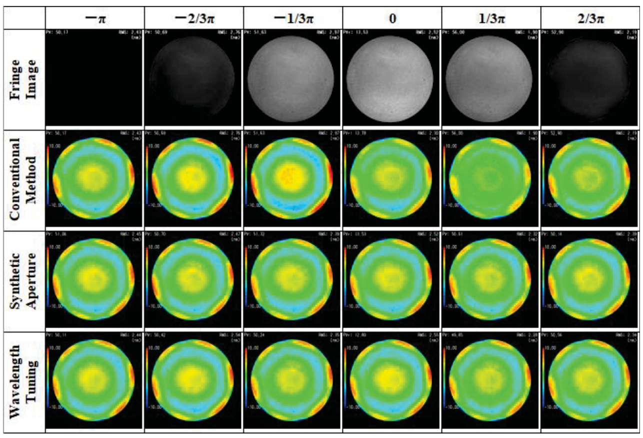


Fig. 2. Raw interference fringes as function of initial phase and corresponding object phase distributions measured by conventional, synthetic aperture, and wavelength tuning methods.

Figure 3 shows the 3rd-order spherical aberration component $Z_8$ as a function of the initial phase of the interference fringes that is equivalent to the 1st Zernike component $Z_0$. In the figure, we can observe that the object phase obtained by the conventional method suffers from spherical aberrations that show a sinusoidal variation with a peak-to-valley (PV) height of 4 nm. In contrast, the object phase calculated from the same interferograms but by the synthetic method does not show any variational aberration. Moreover, spherical aberration is also not observed in the wavelength tuning method.

## 3. Results and Discussion

In the wavelength tuning method, the amount of phase modulation is proportional to the distance between the two interfering surfaces. The modulation is therefore uniform over the aperture when the two spherical surfaces are fixed at the concentric and null-fringe position. The phase measurement error caused by the modulation nonuniformity does not exist in the wavelength tuning measurement. The 3.7-nm dc component of the spherical aberration observed in Fig. 3 is the actual shape deviation of the test surface.

In the conventional monochromatic measurement, the phase modulation suffers from not only geometrical nonuniformity but also extension nonlinearity of the PZT mechanism. The systematic phase error is a periodic function of the object phase $\varphi$ and can be expanded into the series of modulation nonlinearities $\varepsilon_i$ and an average reflection index $R$ as shown in Eq. (1). Typical magnitudes of these parameters are $\varepsilon_1 = -0.5$, $\varepsilon_2 \approx -0.03$, and $R = 0.04$. The leading error terms are then $\varepsilon_1$, $\varepsilon_1^2$, …, $\varepsilon_1^5$, $\varepsilon_2$, $\varepsilon_1 R$, $\varepsilon_1^2 R$, .....

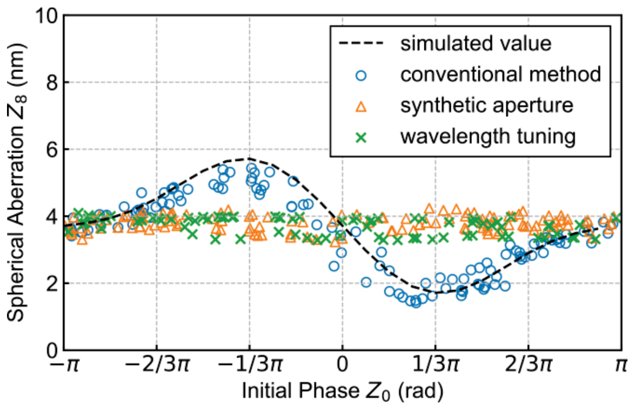


Fig. 3 Spherical aberrations measured by three methods (symbols) and obtained by numerical simulation (dashed curve) as function of initial phase of object.

In the 13-frame algorithm used in the conventional method, all the error coefficients shown in Eq. (1) are designed to be zero. The systematic errors then come from the residual terms of $\varepsilon_1^3$, …, $\varepsilon_1^5$ and $\varepsilon_1^2 R$. In Fig. 3, we can see that the spherical aberration component has a sinusoidal variation and seems proportional to $\sin\varphi$ and $\sin 2\varphi$. Manual calculations show that the leading error terms involving $\varepsilon_1^3$, …, $\varepsilon_1^5$ generally are functions of the even orders of $\varphi$, such as $\sin 2\varphi$, $\sin 4\varphi$, ..., and that the term $\varepsilon_1^2 R$ depends on odd orders of $\varphi$, such as $\sin\varphi$, $\sin 3\varphi$, ... We therefore conclude that the variational spherical aberration component in Fig. 3 are mainly generated by two error terms that are proportional to $\varepsilon_1^2 R$ and $\varepsilon_1^3$.

Strict numerical simulations show that the phase measurement error $\Delta\varphi$ amounts to a PV height of 18 nm for testing a 0.86 NA spherical lens, while the induced 3rd-order spherical aberration component $Z_8$ amounts to a PV height of 4 nm. The experimental results obtained by the conventional method (Fig. 3) are consistent with the simulation results (dashed curve).

Because the former error term of $\varepsilon_1^2 R \sin\varphi$ includes the reflection index $R$, the source of this spherical aberration is mainly inherent to the multiple-reflected beam that travels three times between the two surfaces. The later error term of $\varepsilon_1^3 \sin 2\varphi$ is caused by the spatial deformation of the dominant interference fringes between the two surfaces. Therefore, if the reflection index for the test surface increases, we expect the spherical aberration error, which has no relation to the object shape, to be larger. And similar results are expected for test surfaces with large spherical aberration.

Several approaches can reduce this spherical aberration error. If we apply an ideal Clapham-Dew coating on the reference surface and reduce multiple reflections, we might be able to reduce this aberration. We also have a possibility for a new error-compensating algorithm to eliminate the error coefficient relating to this higher error term. Because the aberration error has a simple sinusoidal dependence on the initial phase of the object, we can eliminate most of the error if we slightly shift the object position, shift the initial object phase two times by $+120^\circ$ and $-120^\circ$, and average the object phases for the three positions.

In contrast to the conventional method, the synthetic method can vary the phase shift increment in the algorithms to $2\pi/N$ rad by varying the divisor as N = 6, 7, …, 12, depending on the position in the aperture. The maximum nonuniformity $\varepsilon_1$ is then reduced from -0.5 to -0.08. Higher-order error terms, such as $\varepsilon_1 R$ and $\varepsilon_1^2 R$, then decrease to 1/6 and 1/39, respectively. This decreases the spherical aberration error significantly, and its magnitude cannot be distinguished from the result obtained by a wavelength tuning measurement.

In conclusion, the phase measurement error caused by the spatial nonuniformity of the phase modulation becomes critical for testing high-NA spherical surfaces with conventional Fizeau interferometers. The magnitude of the induced 3rd-order spherical aberration component $Z_8$ was estimated experimentally by changing the initial phase of the object, which amounted to a PV height of 4 nm when testing a 0.86-NA spherical surface, as an example. However, our new synthetic aperture method can reduce this systematic error without changing any hardware of the interferometer. The validity of the synthetic method was theoretically and experimentally confirmed in the test of a 0.86-NA spherical concave surface. The residual error caused by the synthetic method was found to have a magnitude similar to that of wavelength tuning interferometry.

## REFERENCES

1. R. C. Moore and F. H. Slaymaker, "Direct measurement of phase in a spherical-wave Fizeau interferometer," Appl. Opt. Vol. 19, pp. 2196–2200, 1980.
2. P. de Groot, "Correlated errors in phase-shifting laser Fizeau interferometry," Appl. Opt. Vol. 53, pp. 4334–4342, 2014.
3. T. Kumagai, Y. Nagaike, K. Hibino, and K. Wasaki, "Synthetic aperture phase-shifting interferometry for high-numerical-aperture spherical surface measurement," Opt. Eng. Vol. 60, 014101, 2021.